Electrochimica Acta 60 (2012) 112–120

Contents lists available at SciVerse ScienceDirect

Electrochimica Acta

journal homepage: www.elsevier.com/locate/electacta

Clean hydrogen generation through the electrocatalytic oxidation of formic acid in a Proton Exchange Membrane Electrolysis Cell (PEMEC)

Claude Lamy, Abirami Devadas, Mario Simoes, Christophe Coutanceau *

Laboratory of Electrocatalysis, CNRS UMR 6503, and PACS, CNRS GDR 3339, University of Poitiers, 40 Avenue du Recteur Pineau, 86022 Poitiers Cedex, France

ARTICLE INFO

Article history:
Received 6 July 2011
Received in revised form 31 October 2011
Accepted 2 November 2011
Available online 9 November 2011

Keywords:
Electrolysis
Formic acid
Gold
Hydrogen generation
Pd-based catalysts

ABSTRACT

Several palladium-based electrocatalysts dispersed onto a Vulcan XC-72 carbon support (Pd/C, Pd_xAu_{1-x}/C and Pd_xPt_{1-x}/C) were prepared by the "water-in-oil" microemulsion method and characterized by physicochemical methods (TEM, HRTEM, EDX, XRD, etc.). The electrochemical activity of these catalysts towards the electro-oxidation of formic acid was investigated by cyclic voltammetry, and compared to that obtained with the monometallic catalysts. The electrochemical decomposition of formic acid in a PEMEC at relatively low cell voltages (0.2–0.7 V for a current density of 100 mA cm^{-2} according to the catalyst used) was performed with a much lower electrical energy (1.2–1.6 kWh$(Nm^3\ H_2)^{-1}$ compared to that necessary for water electrolysis (~5 kWh$(Nm^3\ H_2)^{-1}$. Formic acid has been chosen as a model compound with the lowest decomposition energy ($\Delta H \sim 32$ kJ $mole^{-1}$) compared to that needed for water decomposition ($\Delta H \sim 286$ kJ $mole^{-1}$). It has been demonstrated that this technology may allow saving at least two thirds of the electrical energy needed by the classical water electrolysis technology for producing pure hydrogen. Moreover the use of platinum free Pd-based catalysts for the anodic oxidation of formic acid leads to high reaction rates at relatively lower overvoltages, i.e. 0.2–0.4 V at 100 mA cm^{-2}.

1. Introduction

Technological civilization needs more and more energy, particularly in emerging and developing countries. Fossil resources, such as coal, natural gas and hydrocarbons, are the main primary sources, but their amount is limited and will be exhausted in a few decades. Furthermore they are the main contribution to carbon dioxide emission leading to greenhouse effect. An alternative energy source and carrier is hydrogen, which strongly limits the production of greenhouse gases, depending on the primary sources used for its fabrication. Using renewable energy sources, such as nuclear power, hydroelectric power, wind, solar and tidal power, the production of hydrogen by water electrolysis is the most developed process, leading to high purity hydrogen, suitable to feed a low temperature Fuel Cell, such as a PEMFC or an AFC [1].

However due to the high overvoltages encountered in water electrolysis, particularly at the catalytic anode, where oxygen evolution does occur, the production cost is actually not competitive with the main production processes (methane steam reforming, partial oxidation, auto thermal reforming) from natural gas. This is because the energy needed to produce 1 kg of hydrogen is much greater than the theoretical energy (33 kWh kg^{-1} under standard conditions), reaching more than 50 kWh kg^{-1} (corresponding to about 4.5 kWh$(Nm^3\ H_2)^{-1}$, i.e. an energy efficiency less than 67%.

There are 2 ways to decrease this energy amount, either to reduce the overvoltage of the Oxygen Evolution Reaction (OER) by developing more efficient anodic electrocatalysts, or to electrolyze other hydrogen containing compound, such as those derived from the biomass feedstock. The first approach was mainly developed around the world [2–5] leading to commercial electrolyzers [6] with a relatively good energy efficiency (60–70%). Most of the anode catalysts are based on valve oxides (IrO_2, RuO_2, TaO_2) supported on a titanium sheet, similar to DSA type electrodes developed for the chloro-alkali industry. But in the latter case the OER overvoltage was never decreased below 0.4 V (i.e. a cell voltage of 1.6 V) at 1 A cm^{-2} [7].

Therefore the second approach, particularly that using biomass feedstocks as hydrogen sources, is very promising, since the theoretical cell voltage for the electrochemical decomposition of such compounds with hydrogen production is lower than the theoretical cell voltage of water electrolysis (1.23 V under standard conditions). Several compounds from biomass resource, like alcohols, carboxylic acids, sugars, etc., have been be considered as sources of hydrogen, which is mainly produced by thermal catalytic decomposition processes [8–12]. Relatively few works could be found on the electrochemical decomposition of methanol [13–15], glycerol

* Corresponding author.
E-mail address: Christophe.Coutanceau@univ-poitiers.fr (C. Coutanceau).

0013-4686/$ – see front matter © 2011 Elsevier Ltd. All rights reserved.
doi:10.1016/j.electacta.2011.11.006

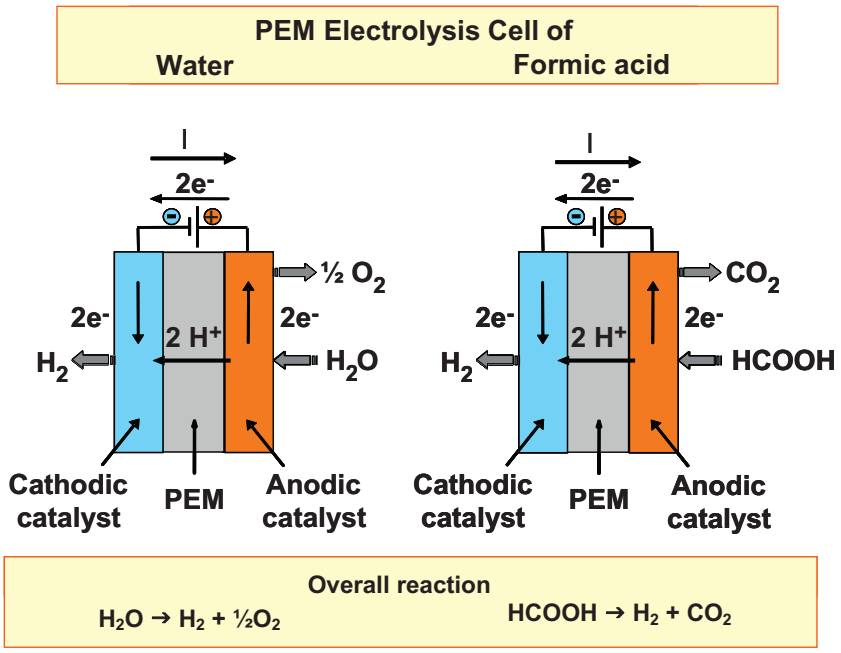

Fig. 1. Schematic principle of the electrochemical decomposition of water and formic acid in a Proton Exchange Membrane Electrolysis Cell (PEMEC).

[16,17], glucose [16] and formic acid [18–20] for hydrogen production. However, in Ref. [18], the chemical approach is not correct, since the authors proposed the following mechanism for the oxidation of formic acid:

$$CH_2O_2 + 1/2O_2 \rightarrow CO_2 + H_2O$$

$$H_2O \rightarrow 1/2O_2 + 2H^+ + 2e^-$$

which is obviously completely wrong from an electrochemical point of view. In their mechanism, the only electrochemical reaction cited is the oxidation of water and not that of formic acid, so that, the electrode potential should be much higher than 1.23 V vs. RHE, even with titanium oxide coated with iridium oxide anodes. Moreover these electrodes are more adapted for water oxidation than for formic acid oxidation. In Ref. [19], Aldous and Compton studied the electrochemical behaviour of HCOOH in a non-aqueous $[NH_4^+][HCOO^-]$ mixture, behaving as a conducting liquid at room temperature. For formic acid oxidation, they obtained performances of ca. 1 mA at + 0.3 V with platinum microelectrodes.

If most of the electrochemical decomposition reactions of these compounds have a low cell voltage (under standard conditions) they lead usually to larger cell voltages, under working conditions, due to high anodic overvoltages. Moreover, studies performed on formic acid oxidative decomposition for hydrogen production did not achieve high current densities, often due to the use of bulk or nanodispersed pure platinum catalyst as anodic electrode, which is not a convenient catalyst for this reaction due to CO surface poisoning.

In this paper the feasibility of the production with higher rate of clean hydrogen by formic acid electrolysis in a Proton Exchange Membrane Electrolysis Cell (PEMEC) has been demonstrated. Formic acid has been chosen as a model compound with the lowest decomposition energy ($\Delta H \sim 32$ kJ mole^{-1} under standard conditions) compared to that needed for water decomposition ($\Delta H \sim 286$ kJ mole^{-1}). Moreover the use of Pd-based catalysts for the anodic oxidation of formic acid lead to high reaction rates at relatively low overvoltages, of the order of 0.2–0.4 V at 100 mA cm^{-2} in a Direct Formic Acid Fuel Cell [21].

1.1. Principle of formic acid decomposition in a PEMEC

The principle of the electrochemical decomposition of formic acid in a PEMEC is similar to that of water (Fig. 1).

In water electrolysis liquid or gaseous water is fed to the anodic compartment where it is oxidized producing oxygen and protons, i.e.:

$$H_2O \rightarrow 1/2O_2 + 2H^+ + 2e^- \quad (1)$$

Oxygen evolves in the gaseous phase, whereas the electrons circulate in the external circuit and protons cross-over the membrane, reaching the cathodic compartment where they are reduced by the electrons coming from the external circuit, thus producing hydrogen, as follows:

$$2H^+ + 2e^- \rightarrow H_2 \quad (2)$$

This corresponds to the overall decomposition of water into hydrogen and oxygen:

$$H_2O \rightarrow H_2 + 1/2O_2 \quad (3)$$

with $\Delta H = 286$ kJ and $\Delta G = 237$ kJ (mole H_2)$^{-1}$ under standard conditions.

Similarly formic acid is fed to the anodic compartment where it is oxidized producing carbon dioxide and protons, i.e.:

$$HCOOH \rightarrow CO_2 + 2H^+ + 2e^- \quad (4)$$

and the protons, which reach the cathodic compartment after crossing-over the membrane, are reduced to hydrogen according to reaction (2).

This corresponds to the overall electrochemical decomposition of formic acid into hydrogen and carbon dioxide, according to:

$$HCOOH \rightarrow H_2 + CO_2 \quad (5)$$

with the thermodynamic data under standard conditions:

$\Delta H = 31.5$ kJ and $\Delta G = -33$ kJ (mole formic acid)$^{-1}$.

Both reactions need external energy ($\Delta H > 0$), coming from the external electrical power sources, but in the case of formic acid the decomposition is spontaneous, since $\Delta G < 0$. The corresponding

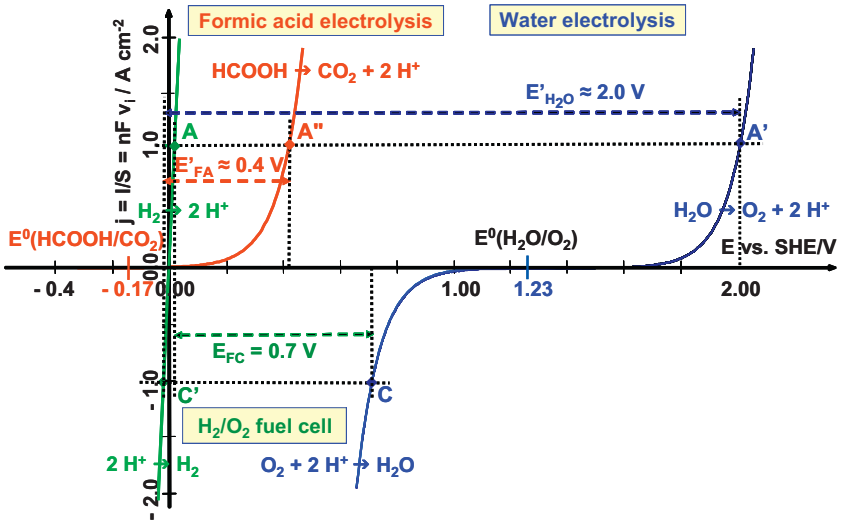

Fig. 2. Comparison of the theoretical $E(j)$ electric characteristics representative of the Butter–Volmer kinetics law for water oxidation, acid formic oxidation, oxygen reduction and proton reduction. (E'_{H_2O}), (E'_{FA}) and (E_{FC}) are the cell voltages for water electrolysis, formic acid electrolysis and hydrogen/oxygen fuel cell at a current density of 1 A cm^{-2}, respectively. $E^\circ(H_2O/O_2) = 1.23$ V/SHE and $E^\circ(HCOOH/CO_2) = -0.17$ V/SHE are the electrochemical reaction standard potentials.

theoretical cell voltage can be calculated from ΔG, i.e. $E_{cell} = \Delta G/2F$, giving respectively:

$E_{cell} = 1.23$ V for water electrolysis and $E_{cell} = -0.17$ V for formic acid decomposition.

However the relatively slow kinetics of the anodic reaction in both processes lead to high anodic overvoltages, greater than 1.8 V in the case of water electrolysis where high current densities (over 1 A cm^{-2}) are necessary for high hydrogen production rates, as shown in Fig. 2. In this figure, the $j(E)$ curves representative of the Butler–Volmer kinetics law are presented for the water oxidation reaction, the formic acid reaction, the hydrogen oxidation reaction (positive current density), the oxygen reduction reaction and the proton reduction reaction (negative current density); from these curves, the cell voltage for water electrolysis (E'_{H_2O}), formic acid electrolysis ($E'_{FA)}$ and hydrogen/oxygen fuel cell (E_{FC}) at a current density of 1 A cm^{-2} can be compared.

In order to get a competitive cost of energy for the production of hydrogen, these overvoltages have to be decreased down to acceptable values. The development of new electrocatalysts is thus highly needed. Indeed, the energy consumed is directly proportional to the cell voltage, according to Eq. (6):

$$W_e\,(\text{in kWh}\left(\text{Nm}^{-3}\,\text{H}_2\right)^{-1}) = \frac{nF}{3600\,V_m \times 10^3} E_{cell}(j) \approx 2.364\,E_{cell}(j) \quad (6)$$

where $V_m = 22.675\,10^{-3}$ m^3 mol^{-1} is the molar volume of an ideal gas at 0 °C, $F = 96{,}485$ C the Faraday constant and n the number of electrons involved in the overall process ($n = 2$ in both cases). Since the electrical energy consumed depends only on the cell voltage $E_{cell}(j)$, where j is the current density, E_{cell} must be below 1 V to decrease the energy below 2.4 kWh (Nm^3)$^{-1}$.

2. Experimental

2.1. Preparation of the catalysts

Catalysts were prepared by mixing $NaBH_4$ (99% from Acros Organics) as a reducing agent, with a microemulsion carrying the corresponding reactants dissolved in an aqueous phase (MilliQ® Millipore, 18.2 MΩ cm): K_2PdCl_4, $H_2PtCl_6{\cdot}6H_2O$ and $HAuCl_4{\cdot}3H_2O$ (from Alfa Aesar, 99.9%) were used. Polyethyleneglycol–dodecylether (BRIJ®30 from Fluka) was chosen as surfactant and the organic phase was n-heptane (99% from Acros Organics). A desired amount of the metal salts was dissolved in ultra-pure water in order to obtain metallic nanoparticles with controlled compositions after the reduction process by $NaBH_4$. Carbon (Vulcan XC72), previously treated under N_2 at 400 °C for 4 h, was added directly in the colloidal solution to obtain the desired metal loading and the mixture was kept under stirring for 2 h. In the present work all the catalysts were synthesized in order to obtain 40 wt% metal loading. The mixture was filtered on a 0.22 μm Durapore® membrane filter (Millipore). The resulting powder was abundantly rinsed with ethanol, acetone and ultra-pure water. The carbon-supported catalysts were dried overnight in an oven at 75 °C.

2.2. Characterization of the Pd-based catalysts

The synthesized catalysts were characterized by differential thermal analysis and thermogravimetric analysis (DTA–TGA), TEM, XRD, inductively coupled plasma optical emission spectroscopy (ICP-OES), and electrochemical methods.

Transmission electron microscopy (TEM) characterization was performed using a Philips CM 120 microscope (120 kV) equipped with a LaB6 filament. The mean particle size and size distribution were determined by measuring the diameter of 200–300 isolated particles using ImageJ free software.

Powder X-ray diffraction (XRD) patterns were recorded on a Bruker D5005 Bragg-Brentano (θ–θ) diffractometer operated with a copper tube powered at 40 kV and 40 mA ($CuK_{\alpha 1} = 1.54060$ Å and $CuK_{\alpha 2} = 1.54443$ Å). Measurements were effectuated from $2\theta = 15°$ to $2\theta = 90°$ in step mode, with steps of 0.06° and a fixed acquisition time of 10 s/step.

For electrochemical characterization, catalytic powders were deposited on a glassy carbon substrate according to a method proposed by Gloaguen et al. [22]. The catalytic powder (25 mg) is added to a mixture of 0.5 mL of Nafion solution (5 wt% from Aldrich) in ultrapure water. After ultrasonic homogenization of the catalyst/XC72-Nafion ink, a given volume is deposited from a syringe onto a fresh polished glassy carbon substrate yielding a catalytic powder loading of 354 μg cm^{-2}. The solvent is then evaporated in a stream of ultrapure nitrogen at room temperature. By this way, a catalytic layer is obtained with a thickness lower than 1 μm.

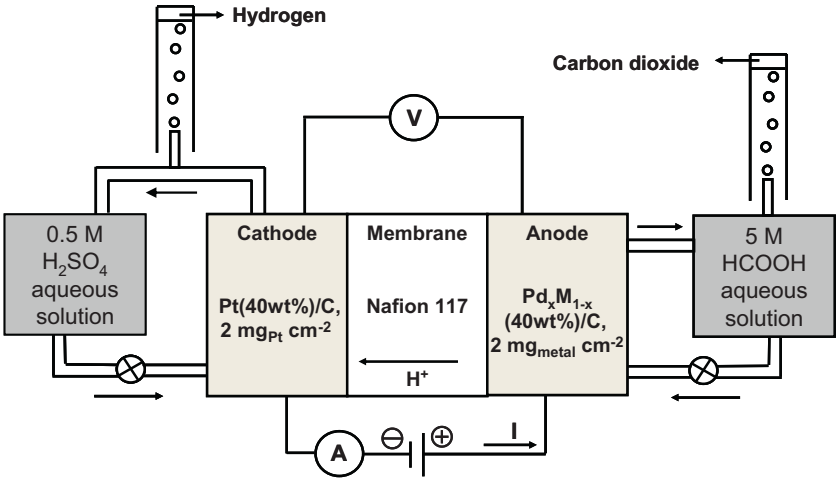

Fig. 3. Experimental set-up for the study of the formic acid electrolysis reaction in a PEMEC and for hydrogen evolution measurements; M = Au or Pt.

The electrochemical setup consists of a Voltalab PGZ 402 computer-controlled potentiostat. The solutions were prepared from 0.5 M H_2SO_4 (suprapur, Merck), 0.01 M formic acid (97%, Alfa Aesar) and ultrapure water. The electrochemical experiments were carried out at 20 °C in N_2-purged supporting electrolyte, using a conventional thermostated three-electrode electrochemical cell. The working electrode was a glassy carbon disk (0.071 cm^2 geometric surface area), the counter electrode was a glassy carbon plate (8 cm^2 geometric surface area), and the reference electrode was a reversible hydrogen electrode (RHE).

2.3. MEA fabrication and electrolysis tests

The electrolysis cell tests in a single PEMEC with a 5 cm^2 geometric surface area were carried out by feeding the anode with formic acid solutions (from 1 M to 10 M) and the cathode with an acidic solution (0.5 M H_2SO_4). The *E*/*t* and *E*/*j* curves were recorded using a high power potentiostat (Wenking model LT 87, Bank Electronik) and a variable resistance in order to fix the current applied to the cell. The volume of generated H_2 was measured by water displacement in a graduated glass tube connected to the cell. The experimental set-up is schematized in Fig. 3.

Electrodes for PEMEC were prepared from an ink consisting of a mixture of Nafion (5 wt% from Aldrich) solution, water and catalytic powder, brushed on a carbon gas diffusion electrode. Carbon gas diffusion electrodes were home-made using a carbon cloth from Electrochem Inc. on which was brushed an ink made of Vulcan XC 72 carbon powder and PTFE dissolved in isopropanol. The gas diffusion electrodes were loaded with 4 mg cm^{-2} of a mixture of carbon powder and 20 wt% PTFE. The metal loading of the electrodes was close to 2.0 mg cm^{-2} and the Nafion loading of the electrode was ca. 0.8 mg cm^{-2}. The MEAs were prepared, by hot pressing at 130 °C for 90 s under a pressure of 35 kg cm^{-2}, a pretreated Nafion 117 membrane with a cathode (2.0 mg cm^{-2} Pt loading, 40 wt% Pt on carbon, 20 wt% PTFE, 0.8 mg cm^{-2} Nafion) and with anodes (2.0 mg cm^{-2} metal loading, 40 wt% metal on carbon, 20 wt% PTFE, 0.8 mg cm^{-2} Nafion).

3. Results and discussion

3.1. Electrocatalytic activity of Pd-based alloys towards the oxidation of formic acid

The main characterization data of monometallic Pd/C and bimetallic Pd_xAu_{1-x}/C catalysts were previously obtained, for others applications [23]. The main information is that the synthesis method led to metal loadings between 35 and 41 wt% as determined by TDA-TGA measurements, which is very close to the nominal one (40 wt%), and that catalyst compositions as determined by ICP-OES are also in agreement with the nominal ones. It was also shown from recorded XRD patterns that the PdAu systems form true alloys (the Vegard's law was respected) and from TEM analyses that the particle size increased monotonously with the Au atomic ratio in the bimetallic catalyst, from ca. 4.0 nm for the Pd/C catalyst to ca. 5.3 nm for the Pd_1Au_9/C nanomaterial. Concerning the PdPt/C catalysts, TEM image of the $Pd_{0.5}Pt_{0.5}$/C materials and the corresponding particle size distribution are given as examples in Fig. 4. Analysis of the TEM results led to a mean particle size of ca. 4.0 nm.

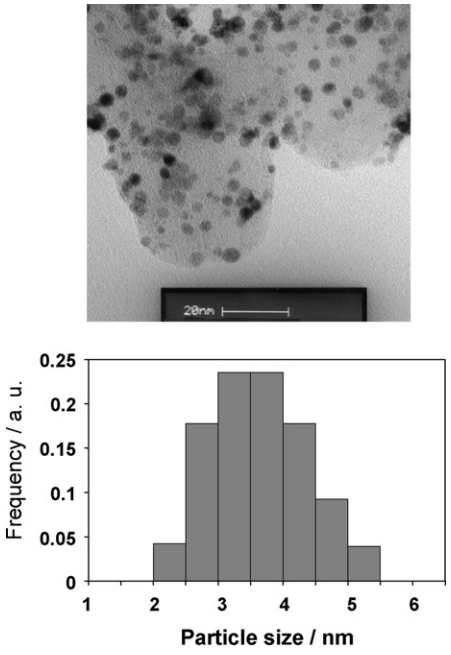

Fig. 4. TEM picture and related particle size distribution of the $Pd_{0.5}Pt_{0.5}$/C catalyst (40 wt% metal loading on Vulcan XC-72 carbon).

In order to choose the best anode catalysts for the electrochemical oxidation of formic acid, cyclic voltammograms were recorded in a 3-electrode cell with several Pd-based electrodes in a 0.5 M H_2SO_4 solution containing 0.01 M HCOOH (Fig. 5). Recent studies have suggested that palladium and palladium-based alloys have

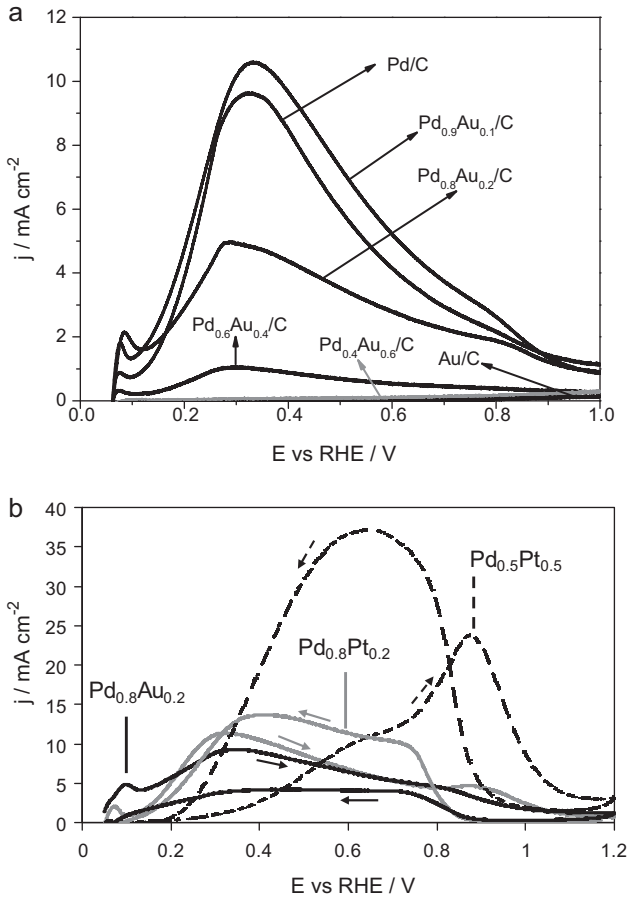

Fig. 5. Voltammetric curves recorded during the oxidation of 10^{-2} M HCOOH in 0.5 M H_2SO_4 N_2-purged electrolyte on (a) different Pd_xAu_{1-x}/C catalysts and (b) comparison of the catalytic activity of Pd_xPt_{1-x} and $Pd_{0.8}Au_{0.2}$/C catalysts (T = 25 °C; v = 50 mV s^{-1}).

interesting activity compared to platinum for the electrooxidation reaction of formic acid [24,25].

Two parallel pathways for the electrooxidation of formic acid in CO_2 were proposed [26–31], both leading to the exchange of 2 electrons per oxidized formic acid molecule. The former reaction occurs without formation of adsorbed CO as intermediate (Eq. (7)), whereas the second one involves the reaction of formic acid on a Pt catalytic site to form a CO intermediate which will be further oxidized to CO_2 (Eqs. (8)–(10)):

Direct reaction pathway

$$Pt_s + HCOOH \rightarrow Pt_s + CO_2 + 2H^+ + 2e^- \quad (7)$$

Indirect reaction pathway

$$Pt_s + HCOOH \rightarrow Pt\text{–}CO + H_2O \quad (8)$$

$$Pt_s + H_2O \rightarrow Pt\text{–}OH + H^+ + e^- \quad (9)$$

$$Pt\text{–}CO + Pt\text{–}OH \rightarrow 2Pt_s + CO_2 + H^+ + e^- \quad (10)$$

where Pt_s represents a platinum catalytic site.

Such mechanisms are expected to occur also on palladium-based catalysts as Lu et al. [32] showed that the addition of palladium to platinum led to enhance the direct reaction pathway.

PdAu or PdPt alloys with a low content of Au or Pt (atomic ratio <20%) display a good electrocatalytic behaviour, in agreement with the results obtained at low overpotentials with a PtPd catalyst in a Direct Formic Acid Fuel Cell by Rice et al. [33], and with different PdAu catalysts in a classical electrochemical cell by Zhang et al. [34]. Particularly the voltammograms of the $Pd_{0.9}Au_{0.1}$ and $Pd_{0.8}Pt_{0.2}$ alloys display the forward and backward sweeps quasi super-imposed. This indicates that these catalytic surfaces are less sensitive to poisoning by adsorbed CO species resulting from the dissociative chemisorption of formic acid. Indeed, on the basis of *in situ* infrared study on glycerol oxidation at Pt(1 0 0) surface, Behrens et al. [35] clearly showed the formation of adsorbed CO species as soon as 0 V vs. RHE, which was proposed to partly explain the deactivation process of platinum catalysts [36].

The electrocatalytic behaviour of $Pd_{0.8}Pt_{0.2}$/C is particularly interesting since the oxidation of formic acid begins at electrode potentials as low as 0.1 V vs. RHE leading to a peak current density of 12 mA cm^{-2} at 0.28 V. Similarly the $Pd_{0.9}Au_{0.1}$/C catalyst gives maximum current densities of about 20 mA cm^{-2} at 0.32 V vs. RHE. Therefore long-term electrolysis of formic acid in a PEMEC was undertaken with the following catalysts: $Pd_{0.8}Au_{0.2}$/C, $Pd_{0.9}Au_{0.1}$/C and $Pd_{0.8}Pt_{0.2}$/C.

3.2. Effect of the concentration of formic acid

In order to determine the best composition of the electrolytic solution (0.5 M H_2SO_4 + x M HCOOH), several concentrations of formic acid were investigated (x = 1 M, 2 M, 5 M and 10 M) at different controlled current densities (40–200 mA cm^{-2}). The cell voltage, U_{cell} at a fixed current density, was recorded as a function of time for 30 min (Fig. 6).

The results obtained with a $Pd_{0.8}Au_{0.2}$/C anode show a quasi-linear variation of U_{cell} with time, with a positive slope. Three potential regions can be observed according to the change in the slopes of the straight line $U_{cell}(t)$, independently of the current density and of the HCOOH concentration: for initial cell voltages lower than 0.5 V, the slopes are low, for initial cell voltages higher than ca. 0.5 V, the slopes increase drastically, and then for 10 M HCOOH U_{cell} remains nearly constant at a high value ($U_{cell} \approx 1$ V). This behaviour can be related with the poisoning process of the catalytic surface by CO species coming from HCOOH adsorption. Behrens et al. [35] showed clearly that the higher CO coverage on a Pt(1 0 0) surface was not achieved at low electrode potentials but in an intermediate potentials range from ca. 0.35 to ca. 0.45 V vs. RHE, and that it drastically decreases for higher potential. It may be that the $Pd_{0.8}Au_{0.2}$/C catalytic surface behaves in the same way, which could explain the high increase of the cell voltage with time for intermediate cell voltage higher than 0.5 V and its constant value for a high cell voltage of 1 V.

For lower concentrations than 10 M, U_{cell} does not display values higher than 0.5 V, except for 5 M HCOOH at a current density of 200 mA cm^{-2}. Therefore in the following experiments the best formic acid concentration was chosen equal to 5 M.

3.3. Determination of the electrical characteristics $U_{cell}(j)$

From the previous curves recorded at several current densities (j = 40, 80, 120, 160 and 200 mA cm^{-2}) it was possible to draw the electrical characteristic $U_{cell}(j)$ curves at the beginning (t = 0) and at the end (t = 30 min.) of the experiment. The curves obtained for the 3 electrocatalysts investigated display different behaviours depending on the second metal added to palladium (Fig. 7).

For all catalysts, the cell voltage was always higher after 30 min electrolysis than the initial values, independently of the current density used. This behaviour is not very interesting for long-term electrolysis, since U_{cell} increases continuously with time, leading to higher electrical energy consumption. Yu and Pickup [37] also observed that the catalytic activity of Palladium-based catalysts decreased quite rapidly under Direct Formic Acid Fuel Cell (DFAFC) operating conditions. But, these authors underlined that the deactivation was caused by the electro-oxidation of formic acid, and that it was possible to reactivate the catalysts by driving the cell

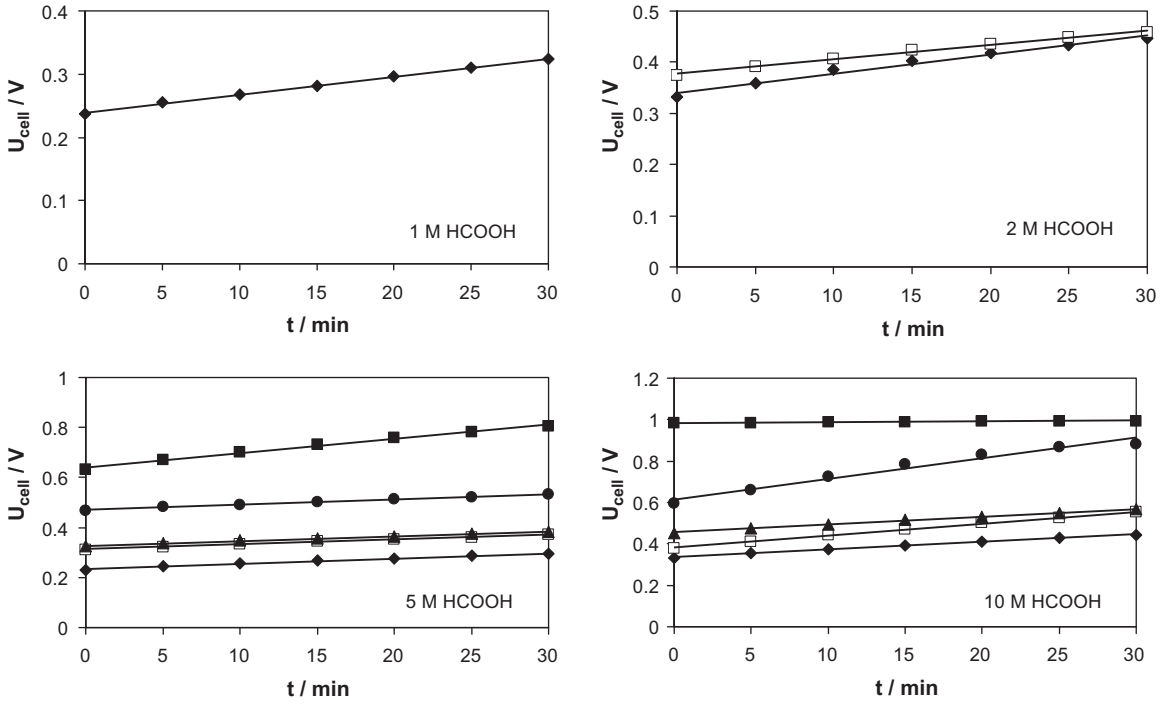

Fig. 6. Electrolysis cell voltage vs. time at 25 °C for a PEMEC using $Pd_{0.8}Au_{0.2}$/C and Pt/C electrodes, 0.5 M H_2SO_4 with several concentrations of formic acid (1 M, 2 M, 5 M and 10 M); (♦) j = 40 mA cm^{-2}, (□) j = 80 mA cm^{-2}, (●) j = 120 mA cm^{-2}, (▲) j = 160 mA cm^{-2} and (■) j = 200 mA cm^{-2}.

voltage to a reverse polarity of −0.2 V. This means that the anode potential, where HCOOH oxidation reaction occurred, was held at an electrode potential 0.2 V higher than that of the oxygen cathode of the Direct Formic Acid Fuel Cell, i.e. to a very high potential (close to ca. 0.9–1.0 V vs. RHE). Under such anode potential conditions, previously adsorbed CO from HCOOH is oxidized, and in the same time either no adsorbed CO is formed from HCOOH adsorption, or the adsorbed CO oxidation kinetics is too high to lead to surface accumulation and blocking. Therefore, such treatment makes the catalyst surface clean. One can notice that this explanation

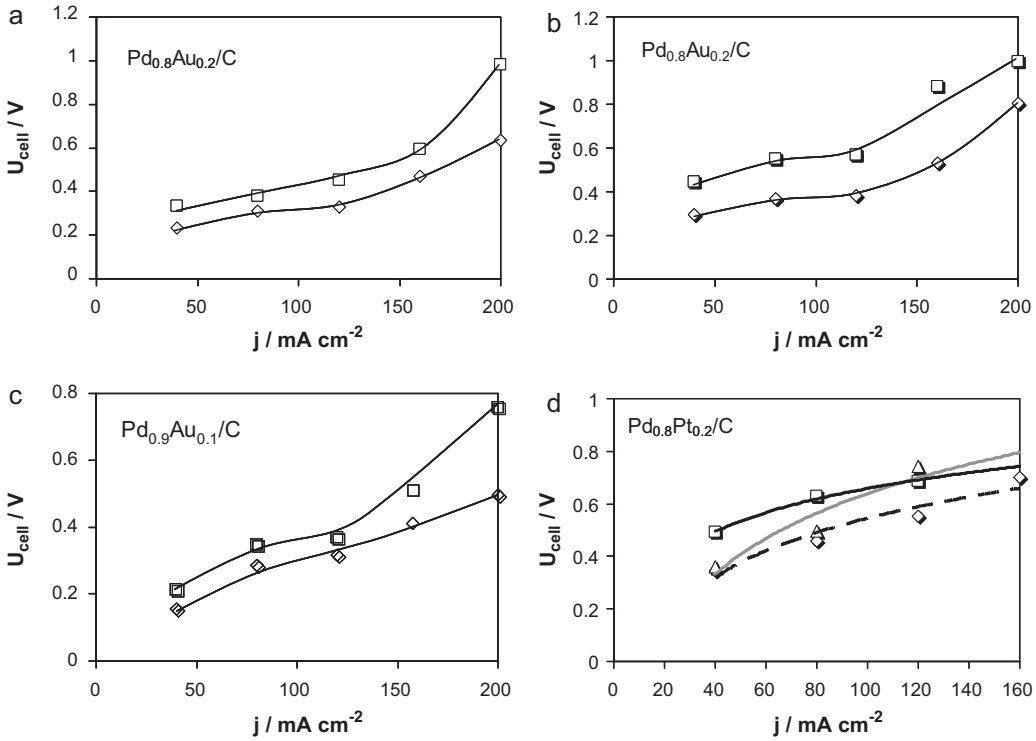

Fig. 7. Electrolysis cell voltage vs. current density for the oxidation of y M HCOOH in the PEMEC (0.5 M H_2SO_4, Pt/C, N117, Pd_xM_{1-x}/C, y M HCOOH) at 25 °C. (a) initial cell voltage and (b) cell voltage after 30 min electrolysis with $Pd_{0.8}Au_{0.2}$/C of 5 M HCOOH (◊) and 10 M HCOOH (□) (c) initial cell voltage (◇) and cell voltage after 30 min electrolysis □) of 5 M HCOOH with $Pd_{0.9}Au_{0.1}$/C and (d) cell voltage after 30 min electrolysis of 2 M HCOOH (△), 5 M HCOOH (◊) and 10 M HCOOH (□) with $Pd_{0.8}Pt_{0.2}$.

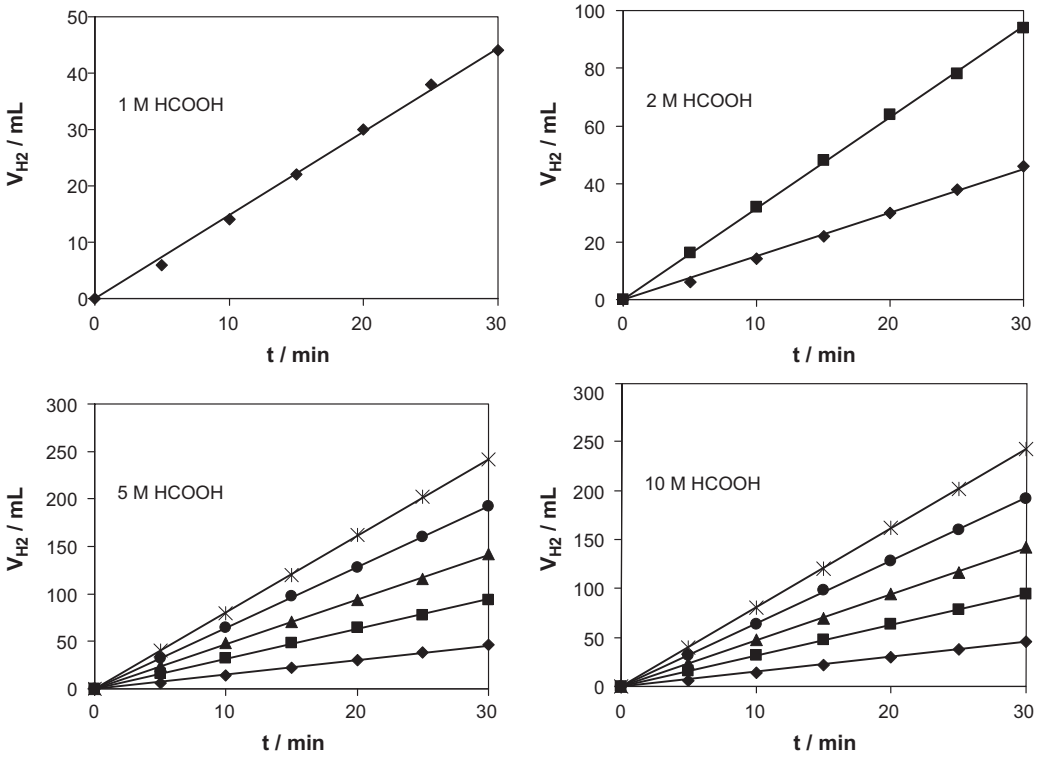

Fig. 8. Hydrogen evolution at different current density for the PEMEC (0.5 M H_2SO_4, Pt/C, N117, $Pd_{0.8}Au_{0.2}$/C, *x* M HCOOH) at 25 °C. (♦) $j = 40\ mA\ cm^{-2}$, (■) $j = 80\ mA\ cm^{-2}$, (▲) $j = 120\ mA\ cm^{-2}$, (●) $j = 160\ mA\ cm^{-2}$ and (⋆) $j = 200\ mA\ cm^{-2}$.

Table 1
Summary of the results obtained in a PEMEC for the different catalysts at 25 °C for [HCOOH] = 5 M.

I/A	Theoretical values		$dV/dt_{(average)}$/cm³ min⁻¹			$V_{H_2}(30')$experimental/cm³		
	dV/dt/cm³ min⁻¹	$V_{H_2}(30')$/cm³	$Pd_{0.9}Au_{0.1}$	$Pd_{0.8}Au_{0.2}$	$Pd_{0.8}Pt_{0.2}$	$Pd_{0.9}Au_{0.1}$	$Pd_{0.8}Au_{0.2}$	$Pd_{0.8}Pt_{0.2}$
0.2	1.52	46	1.51	1.51	1.51	46	46	46
0.4	3.04	92	3.17	3.15	3.2	94	94	96
0.6	4.56	137	4.78	4.70	4.70	144	142	142
0.8	6.09	183	6.40	6.41	6.41	192	192	192
1.0	7.61	228	8.05	8.07	Oscillation[a]	242	242	Oscillation[a]

[a] The oscillation of the cell voltage may result from the formation of adsorbed CO and its fast oxidation, as it was previously observed for the formic acid oxidation at a rhodium electrode [38].

is in agreement with the constant value of U_{cell} observed at 1 V (Fig. 6c).

For the gold containing electrodes ($Pd_{0.8}Au_{0.2}$/C and $Pd_{0.9}Au_{0.1}$/C) the cell voltage, after 30 min electrolysis, seems to reach a first plateau at 0.35 V (for 5 M HCOOH) with current densities in the range 75–125 $mA\ cm^{-2}$, then the cell voltage increases continuously reaching 1.0 V at 200 $mA\ cm^{-2}$ (Fig. 7a–c). Conversely with the $Pd_{0.8}Pt_{0.2}$/C electrode (Fig. 7d) the $U_{cell}(j)$ curves for different HCOOH concentrations (2, 5 and 10 M) tend to a limiting value close to 0.7 V after 30 min electrolysis. Such behaviour could be expected from the cyclic voltammograms recorded in the presence of 10^{-2} M HCOOH. One can see indeed in Fig. 5 that the activity in terms of the achieved current density of Au containing Pd catalysts continuously decreases from electrode potentials higher than ca. 0.4 V vs. RHE, whereas the Pt containing catalyst display its higher catalytic activity in a higher electrode potential range from ca. 0.8 V to 1.0 V vs. RHE.

3.4. Measurement of the hydrogen evolution rate

The hydrogen evolution rate was determined by measuring the volume of evolved hydrogen as a function of time for the different current densities ($j = 40, 80, 120, 160$ and $200\ mA\ cm^{-2}$) at different concentrations (1 M, 2 M, 5 M and 10 M) of formic acid (see Fig. 3).

In all experiments the measured volume of hydrogen is a linear function of time (with correlation coefficients > 0.9986) showing clearly that the volume of evolved hydrogen does not depend on HCOOH concentration, nor on the nature of the electrode catalyst, but only on the current intensity *I* (Fig. 8).

This proves that the process follows the Faraday law according to the following equations:

$$\frac{dV_{H_2}}{dt} = \frac{V_{mol}dN_{H_2}}{dt} = V_{mol}\left(\frac{I}{nF}\right) \quad (11)$$

$$\frac{dV_{H_2}}{dt} = V_{mol}\left(\frac{I}{2F}\right) \times 60 = 7.61\,(I)\ \text{in}\ cm^3\ min^{-1} \quad (12)$$

where V_{mol} is the molar volume of hydrogen at a given temperature and pressure ($V_{mol} = 24.465\ 10^{-3}\ m^3\ mol^{-1}$ at 25 °C and 1 bar), and $n = 2$ is the number of electrons involved in the oxidation reaction of a formic acid molecule according to Eq. (7) (direct oxidation mechanism) or to Eqs. (8)–(10) (indirect reaction mechanism).

Table 1 summarizes all the results obtained with the 3 electrocatalysts ($Pd_{0.8}Au_{0.2}$/C, $Pd_{0.9}Au_{0.1}$/C and $Pd_{0.8}Pt_{0.2}$/C) investigated here, where $dV/dt_{(average)}$ is the average value calculated with all

Table 2
Summary of the results for $Pd_{0.9}Au_{0.1}$/C at 25 °C for [HCOOH] = 5 M; U_{cell} is the PEMEC voltage and W_e is the electrical energy.

I/A	$U_{cell(t=0)}$/V	$W_{e(t=0)}$/ kWh(Nm^3 H_2)$^{-1}$	$U_{cell(t=30')}$/V	$W_{e(t=30')}$/ kWh(Nm^3 H_2)$^{-1}$
0.2	0.156	0.37	0.214	0.51
0.4	0.227	0.54	0.347	0.82
0.6	0.315	0.74	0.369	0.87
0.8	0.411	0.97	0.507	1.20
1.0	0.496	1.17	0.756	1.79

Table 3
Summary of the results for $Pd_{0.8}Au_{0.2}$/C at 25 °C for [HCOOH] = 5 M; U_{cell} is the PEMEC voltage and W_e is the electrical energy.

I/A	$U_{cell(t=0)}$/V	$W_{e(t=0)}$/ kWh(Nm^3 H_2)$^{-1}$	$U_{cell(t=30')}$/V	$W_{e(t=30')}$/ kWh(Nm^3 H_2)$^{-1}$
0.2	0.231	0.55	0.295	0.70
0.4	0.312	0.74	0.370	0.87
0.6	0.327	0.77	0.384	0.91
0.8	0.468	1.10	0.531	1.26
1.0	0.633	1.50	0.806	1.90

Table 4
Summary of the results for $Pd_{0.8}Pt_{0.2}$/C at 25 °C for [HCOOH] = 5 M: U_{cell} is the PEMEC voltage and W_e is the electrical energy.

I/A	$U_{cell(t=0)}$/V	$W_{e(t=0)}$/ kWh $(Nm)^{-3}$	$U_{cell(t=30')}$/V	$W_{e(t=30')}$/ kWh $(Nm)^{-3}$
0.2	0.265	0.62	0.343	0.81
0.4	0.346	0.81	0.459	1.08
0.6	0.439	0.103	0.553	1.30
0.8	0.563	1.32	0.699	1.64
1.0	Unstable		Unstable	

the concentration (1–10 M) of formic acid. The experimental results are compared to the calculated values of dV_{H_2}/dt, the theoretical slope of the $V_{H_2}(30')$ after 30 min electrolysis. The agreement is very good in all experiments, but with experimental values slightly higher than those calculated, which may come from the room temperature a little bit higher than 25 °C. This positive deviation in the measured volume of evolved hydrogen could also be due to resistive heating in the cell during long term electrolysis leading to an increase of the temperature of the exhaust gas.

For all experiments the electrical energy needed to produce 1 Nm^3 of hydrogen was also evaluated, since it is only a function of the cell voltage U_{cell}, according to Eq. (6). The values obtained for U_{cell} at 30 min electrolysis are given in Tables 2–4.

In all the results obtained the amount of electrical energy is below 2 kWh(Nm^3 H_2)$^{-1}$ (since U_{cell} < 0.9 V), which is at least 2 and half times lower than the energy consumed for water electrolysis.

4. Conclusions

Beside water many other hydrogen containing compounds, in particular organic compounds, can generate hydrogen through their dissociation.

The electrochemical decomposition of water or organic compounds gives much more pure hydrogen than thermal processes such as SR, ATR and PrOx. Water electrolysis is a nearly mature process, but it needs a relatively high amount of energy (~5 kWh(Nm^{-3} H_2)$^{-1}$.

In this work, we gave some insights on the feasibility of the production of clean hydrogen by the electrolysis of organic compounds, such as formic acid, in a Proton Exchange Membrane Electrolysis Cell (PEMEC):

- The thermodynamic characteristics of formic acid decomposition (E_{cell} = −0.17 V) make this organic compound a convenient model molecule for PEMEC;
- Pd-based catalysts are active and stable for the anodic oxidation of formic acid;
- High reaction rates at relatively low overvoltages, i.e. 0.2–0.4 V at 100 mA cm^{-2}, have been achieved in a PEMEC with platinum free Pd-based catalysts;
- More than two thirds of the electrical energy can be saved with formic acid decomposition in a PEMEC when compared to water;
- Performance degradation of Pd-based catalysts is at least partly due to catalyst deactivation by CO-poisoning.

To go further, Pd-based electrocatalysts investigated in this work must be improved in terms of performance and stability. Development of more active and stable catalysts for the electrooxidation of organics is needed. The working current density has to be increased above 0.5 A cm^{-2}, keeping low cell voltages in order to make the system competitive with the water electrolysis process. The stability of the catalyst has to be improved for long-time experiments, in particular but not only, has the tolerance towards CO poisoning, which contributes to performance degradation over time, to be improved.

Acknowledgements

The authors greatly acknowledge the CNRS Research Grouping PACS (GDR 3339) and the Institute of Chemistry of the "Centre National de la Recherche Scientifique" (CNRS) for supporting this work. Two of us (A.D. and M.S.) thank the "Agence Nationale de la Recherche" (ANR) through the BODIPAC project for postdoctoral and doctoral fellowships, respectively.

References

[1] B. Sørensen, Hydrogen and Fuel Cell Emerging Technologies and Applications, Elsevier Academic Press, New York, 2005.
[2] S. Grigoriev, V. Porembsky, V. Fateev, Int. J. Hydrogen Energy 31 (2006) 171.
[3] Y. Nishimura, K. Yasuda, Z. Siroma, K. Asaka, Denki Kagaku Oyobi Kogyo Butsuri Kagaku 65 (1997) 1122.
[4] P. Millet, F. Andolfatto, R. Durand, Int. J. Hydrogen Energy 21 (1996) 87.
[5] A. Marshall, Characterisation of electrocatalysis for water electrolysis, Ph.D. Thesis, NTNU, Trondheim, Norway, 2005.
[6] K.E. Ayers, C. Capuano, B. Carter, L. Dalton, G. Hanlon, J. Manco, M. Niedzwiecki, Polymer Electrolyte Fuel Cells 10 Symposium, 218th ECS Meeting, Las Vegas, NV, October 10–15, 2010, Abstract 603.
[7] A. Marshall, S. Sunde, M. Tsypkin, R. Tunold, Int. J. Hydrogen Energy 32 (2007) 2320.
[8] A. Tanksale, J.N. Beltramini, G. Qing, M. Lu, Renew. Sustain. Energy Rev. 14 (2010) 166.
[9] S. Therdthianwong, N. Srisiriwat, A. Therdthianwong, E. Croiset, J. Supercrit. Fluids 57 (2011) 58.
[10] M. Ni, D.Y.C. Leung, M.K.H. Leung, Int. J. Hydrogen Energy 32 (2007) 3238.
[11] A.F. Ghenciu, Curr. Opin. Solid State Mater. Sci. 6 (2002) 389.
[12] D.A. Bulushev, S. Beloshapkin, J.R.H. Ross, Catal. Today 154 (2010) 7.
[13] T. Take, K. Tsurutani, M. Umeda, J. Power Sources 164 (2007) 9.
[14] Z. Hu, M. Wu, Z. Wei, S. Song, P.K. Shen, J. Power Sources 166 (2007) 458.
[15] S.R. Narayanan, W. Chun, B. Jeffries-Nakamura, T.I. Valdez, US Patent 6,533,919, March 18, 2003.
[16] P.A. Selembo, J.M. Perez, W.A. Lloyd, B.E. Logan, Int. J. hydrogen energy 34 (2009) 5373.
[17] A.T. Marshall, R.G. Haverkamp, Int. J. Hydrogen Energy 33 (2008) 4649.
[18] E.Ö. Kiliça, A.S. Koparal, Ü.B. Öğütveren, Fuel Process. Technol. 90 (2009) 158.
[19] L. Aldous, R.G. Compton, Energy Environ. Sci. 3 (2010) 1587.
[20] W.L. Guo, L. Li, L.L. Li, S. Tian, S.L. Liu, Y.P. Wu, Int. J. Hydrogen energy 36 (2011) 9415.
[21] R. Larsen, S. Ha, J. Zakzeski, R.I. Masel, J. Power Sources 157 (2006) 78.
[22] F. Gloaguen, N. Andolfatto, R. Durand, P. Ozil, J. Appl. Electrochem. 24 (1994) 863.
[23] M. Simões, S. Baranton, C. Coutanceau, J. Phys. Chem. C 113 (2009) 13369.
[24] V. Mazumder, S. Sun, J. Am. Chem. Soc. 131 (2009) 4588.
[25] W. Zhou, J.Y. Lee, Electrochem. Commun. 9 (2007) 1725.
[26] A. Capon, R. Parsons, J. Electroanal. Chem. 44 (1973) 239.
[27] B. Beden, C. Lamy, in: R.J. Cale (Ed.), Spectroelectrochemistry, Theory and Practice, Plenum Press, New York, 1988.

[28] X. Xia, T.J. Iwasita, J. Electrochem. Soc. 140 (1993) 2559.
[29] N. Markovic, H. Gaseiger, P. Ross, X. Jian, I. Villegas, M. Weaver, Electrochim. Acta 40 (1995) 91.
[30] T.D. Jarvi, E.M. Stuve, in: J. Lipkowski, P.N. Ross (Eds.), Fundamental Aspects of Vacuum and Electrocatalytic Reactions of Methanol and Formic Acid on Platinum Surfaces, Wiley, New York, 1998.
[31] P.N. Ross, in: J. Lipkowski, P.N. Ross (Eds.), The Science of Electrocatalysis on Bimetallic Surfaces, Wiley, New York, 1998, p. 63.
[32] G.Q. Lu, A. Crown, A. Wieckowski, J. Phys. Chem. B 103 (1999) 9700.
[33] C. Rice, S. Ha, R.I. Masel, A. Wieckowski, J. Power Sources 115 (2003) 229.
[34] G. Zhang, Y. Wang, X. Wang, Y. Chen, Y. Zhou, Y. Tang, L. Lu, J. Bao, T. Lu, Appl. Catal. B: Environ. 102 (2011) 614.
[35] R.L. Behrens, A. Lagutchev, D.D. Dlott, A. Wieckowski, J. Electroanal. Chem. 649 (2010) 32.
[36] X. Yu, P.G. Pickup, Electrochem. Commun. 11 (2009) 2012.
[37] X. Yu, P.G. Pickup, J. Power Sources 187 (2009) 493.
[38] A. Bewick, B. Beden, C. Lamy, J. Electroanal. Chem. 121 (1981) 115.